

Supporting Information

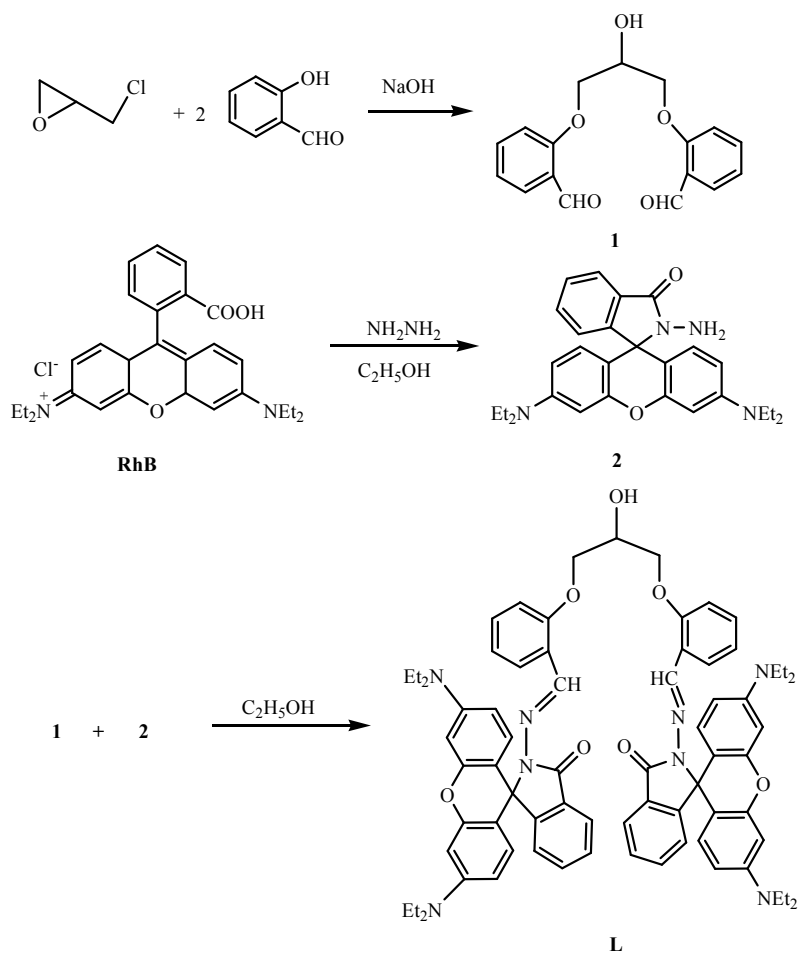
A New Fluorescent Rhodamine B Derivative as “Off-On” Chemosensor for Cu(II) with High Selectivity and Sensitivity

Xianfu Meng, Yanxia Xu, Jinliang Liu*, Lining Sun, and Liyi Shi*

Research Center of Nano Science and Technology, Shanghai University, 200444, China.

* Corresponding authors.

E-mail addresses: liujl@shu.edu.cn; shiliyi@shu.edu.cn.



Scheme S1. The synthesis procedure of DFPP (1), RhB-NH₂ (2), and DFPP-RhB (L).

Table 1. Crystal data and structure refinement for DFPP-RhB.

Identification code	DFPP-RhB	
Empirical formula	C ₇₅ H ₈₀ Cl ₄ N ₈ O ₇	
Formula weight	1347.27	
Temperature	203(2) K	
Wavelength	0.71073 Å	
Crystal system	Triclinic	
Space group	P -1	
Unit cell dimensions	a = 11.852(2) Å	a = 102.763(3) Å
	b = 17.309(3) Å	b = 90.722(3) Å
	c = 18.485(4) Å	g = 94.945(3) Å
Volume	3682.9(12) Å ³	
Z	2	
Density (calculated)	1.215 Mg/m ³	
Absorption coefficient	0.218 mm ⁻¹	
F(000)	1420	
Crystal size	0.700 x 0.700 x 0.650 mm ³	
Theta range for data collection	1.461 to 25.150 Å	
Index ranges	-14 ≤ h ≤ 14, -20 ≤ k ≤ 19, -15 ≤ l ≤ 22	
Reflections collected	21641	
Independent reflections	13018 [R(int) = 0.0348]	
Completeness to theta = 25.242?	97.7 %	
Absorption correction	Semi-empirical from equivalents	
Max. and min. transmission	0.745 and 0.620	
Refinement method	Full-matrix least-squares on F ²	
Data / restraints / parameters	13018 / 36 / 894	
Goodness-of-fit on F ²	1.233	
Final R indices [I > 2σ(I)]	R1 = 0.1058, wR2 = 0.3019	
R indices (all data)	R1 = 0.1383, wR2 = 0.3355	
Extinction coefficient	n/a	
Largest diff. peak and hole	1.504 and -1.208 e.Å ⁻³	

Table 2. Bond lengths (Å) and angles (deg) for DFPP-RhB

Bond lengths (Å) and angles (deg) for DFPP-RhB					
N(1)-C(10)	1.379(5)	C(74)-Cl(1)	1.678(8)	C(32)-C(33)	1.485(9)
N(1)-N(2)	1.382(4)	C(74)-Cl(2)	1.750(8)	C(34)-C(35)	1.527(6)
N(1)-C(17)	1.511(5)	C(68)-C(69)	1.503(14)	C(36)-C(37)	1.499(6)
N(2)-C(9)	1.283(5)	C(68')-C(69')	1.496(16)	C(39)-C(40)	1.378(5)
N(3)-C(21)	1.378(5)	C(3)-C(4)	1.397(6)	C(39)-C(44)	1.395(5)
N(3)-C(30)	1.436(7)	C(3)-C(8)	1.399(5)	C(40)-C(41)	1.398(7)
N(3)-C(32)	1.453(7)	C(4)-C(5)	1.370(7)	C(41)-C(42)	1.379(7)
N(4)-C(26)	1.365(5)	C(5)-C(6)	1.383(7)	C(42)-C(43)	1.367(6)
N(4)-C(34)	1.462(5)	C(6)-C(7)	1.380(6)	C(43)-C(44)	1.400(6)
N(4)-C(36)	1.473(5)	C(7)-C(8)	1.395(6)	C(44)-C(45)	1.470(5)
N(5)-N(6)	1.380(4)	C(8)-C(9)	1.469(5)	C(46)-C(47)	1.479(6)
N(5)-C(46)	1.391(5)	C(10)-C(11)	1.468(6)	C(47)-C(52)	1.374(5)
N(5)-C(53)	1.488(5)	C(11)-C(12)	1.385(6)	C(47)-C(48)	1.379(6)
N(6)-C(45)	1.274(5)	C(11)-C(16)	1.391(6)	C(48)-C(49)	1.380(7)
N(7)-C(57)	1.392(7)	C(12)-C(13)	1.400(7)	C(49)-C(50)	1.395(7)
N(7)-C(66)	1.440(7)	C(13)-C(14)	1.374(7)	C(50)-C(51)	1.375(6)
N(7)-C(68')	1.495(18)	C(14)-C(15)	1.380(6)	C(51)-C(52)	1.393(6)
N(7)-C(68)	1.546(12)	C(15)-C(16)	1.386(6)	C(52)-C(53)	1.519(5)
N(8)-C(62)	1.373(5)	C(16)-C(17)	1.513(5)	C(53)-C(65)	1.503(5)
N(8)-C(70)	1.440(6)	C(17)-C(29)	1.508(5)	C(53)-C(54)	1.514(5)
N(8)-C(72)	1.463(6)	C(17)-C(18)	1.516(5)	C(54)-C(59)	1.389(5)
O(2)-C(3)	1.360(5)	C(18)-C(23)	1.378(5)	C(54)-C(55)	1.394(6)
O(2)-C(2)	1.442(5)	C(18)-C(19)	1.396(5)	C(55)-C(56)	1.365(7)
O(3)-C(10)	1.226(5)	C(19)-C(20)	1.379(6)	C(56)-C(57)	1.414(7)
O(4)-C(23)	1.377(4)	C(20)-C(21)	1.407(6)	C(57)-C(58)	1.392(6)
O(4)-C(24)	1.394(4)	C(21)-C(22)	1.405(6)	C(58)-C(59)	1.377(6)
O(5)-C(39)	1.368(5)	C(22)-C(23)	1.391(5)	C(60)-C(65)	1.383(5)
O(5)-C(38)	1.427(5)	C(24)-C(29)	1.371(5)	C(60)-C(61)	1.391(5)
O(6)-C(46)	1.217(5)	C(24)-C(25)	1.390(5)	C(61)-C(62)	1.396(6)
O(7)-C(59)	1.380(4)	C(25)-C(26)	1.399(5)	C(62)-C(63)	1.410(6)
O(7)-C(60)	1.387(5)	C(26)-C(27)	1.425(5)	C(63)-C(64)	1.389(6)
C(1)-O(1)	1.409(6)	C(27)-C(28)	1.354(6)	C(64)-C(65)	1.388(5)
C(1)-C(38)	1.481(7)	C(28)-C(29)	1.406(5)	C(66)-C(67)	1.461(8)
C(1)-C(2)	1.494(7)	C(30)-C(31)	1.586(10)	C(70)-C(71)	1.520(7)
C(72)-C(73)	1.515(8)	C(75)-Cl(4)	1.701(9)	C(75)-Cl(3)	1.708(9)

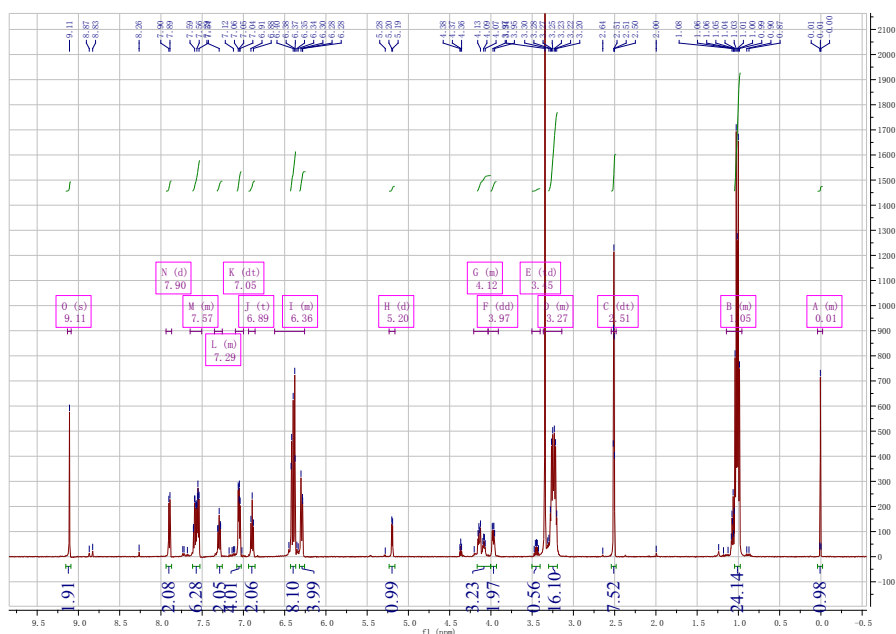


Figure S1. ^1H NMR spectra of DFPP-RhB (DMSO- d_6).

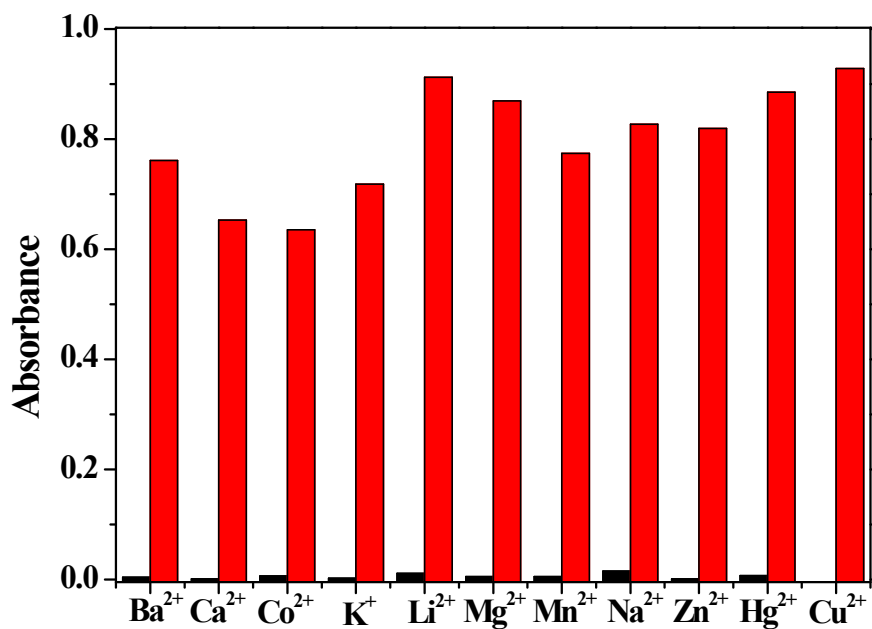


Figure S2. Absorbance changes at 552 nm of DFPP-RhB (10 μM) towards different metal ions (20 μM) in ethanol solution. Dark bars represent the response of DFPP-RhB towards the metal ions of interest, red bars represent the subsequent addition of Cu^{2+} (10 μM) to the above solution.

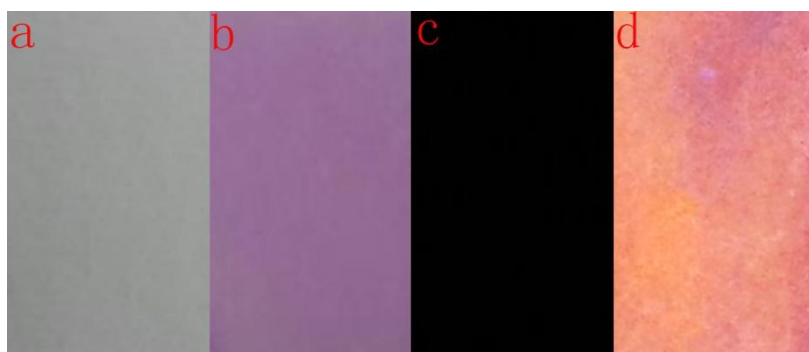


Figure S3. The test paper of DFPP-RhB (a) and after the addition of Cu^{2+} (b) in the bright field; The test paper of DFPP-RhB (c) and after the addition of Cu^{2+} (d) under excitation with UV light at 365 nm.

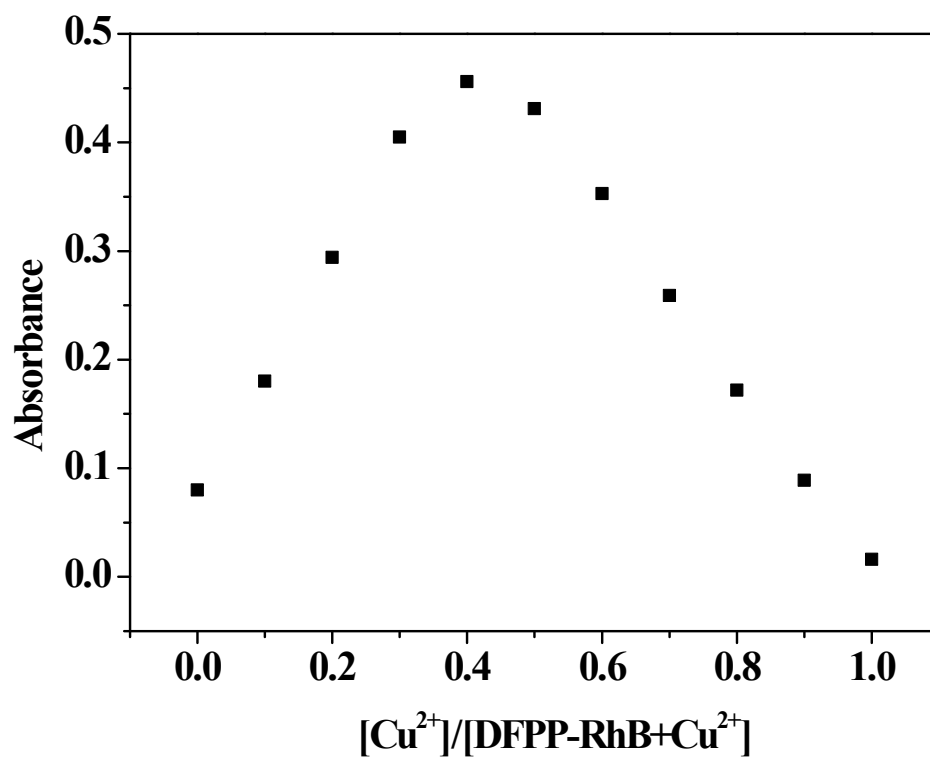


Figure S4. The Job's Plot curve of DFPP-RhB and Cu^{2+} . The total concentration of DFPP-RhB and Cu^{2+} was kept constantly at $10\mu\text{M}$.

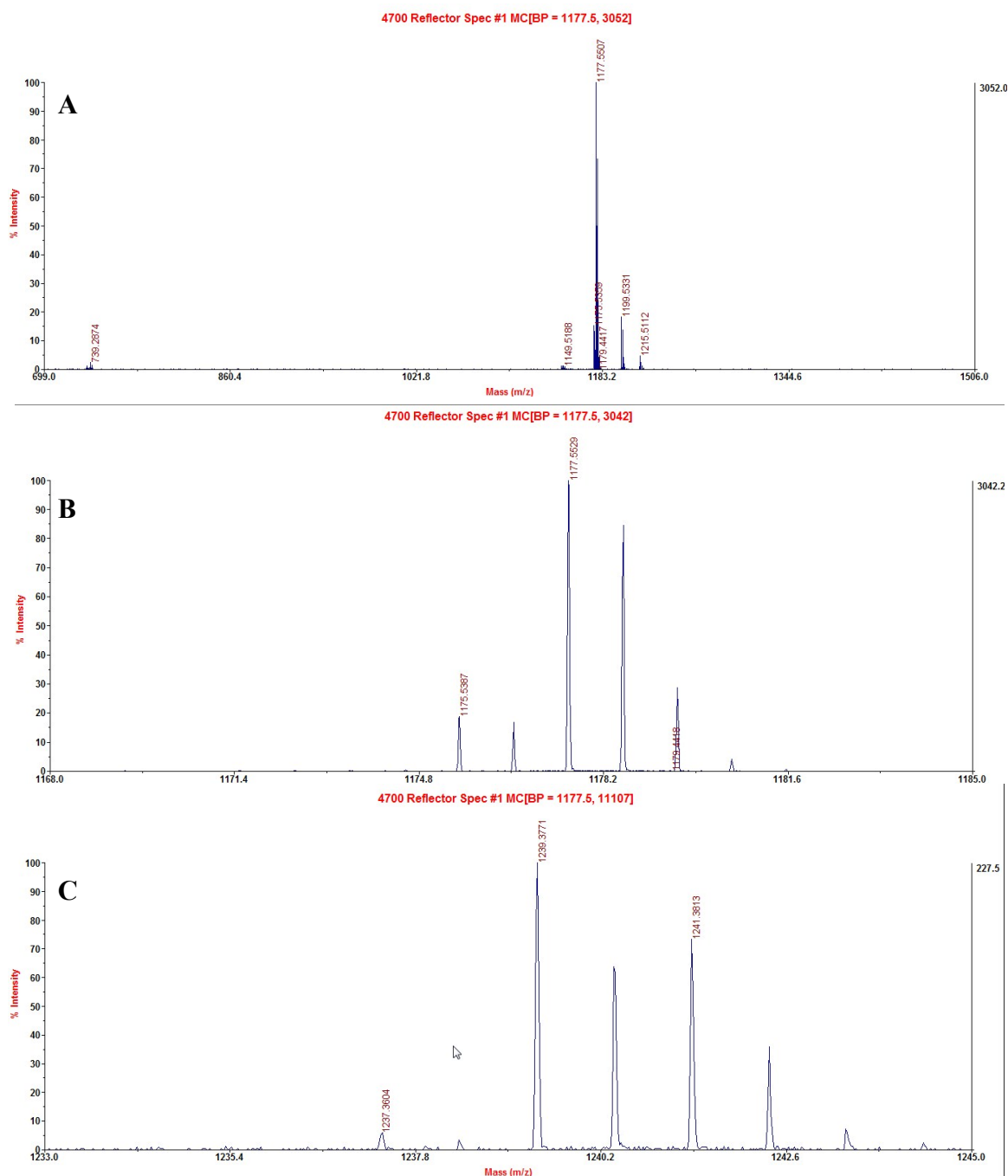


Figure S5. The ESI mass spectra of DFPP-RhB (10 μ M) in the absence (A and B) and presence (C) of Cu^{2+} (20 equiv).

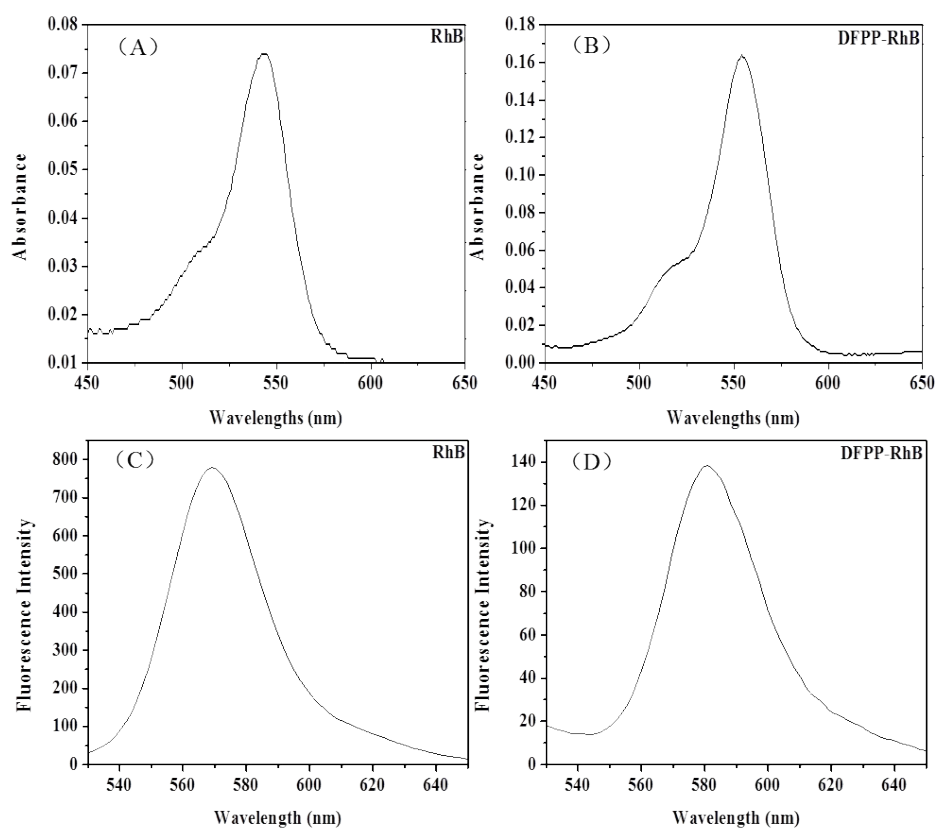


Figure S6. The absorbance spectra of RhB (A) and DFPP-RhB (B), and the fluorescence spectra of RhB (C) and DFPP-RhB (D). The concentration of RhB or DFPP-RhB is 10^{-6} M in absolute ethyl alcohol solution. The fluorescence quantum yield of DFPP-RhB relative to rhodamine B (RhB) was calculated according to the following equation:

$$Q=Q_R \times (I/I_R) \times (A_R/A) \times (\eta^2/\eta_R^2)$$

where Q_R is the quantum yield of the standard (here is RhB), A and A_R are the absorbance of the DFPP-RhB and RhB solution respectively, I and I_R are the emission intensity integration of the DFPP-RhB and RhB solution respectively, and η and η_R are the average refractive index of the solution. Because the both solvents of solution are absolute ethyl alcohol, so the equation is simplified to that:

$$Q=Q_R \times (I/I_R) \times (A_R/A)$$

According to the absorption and emission spectra of RhB and DFPP-RhB, the quantum yield of DFPP-RhB is calculated to be 7.87%.

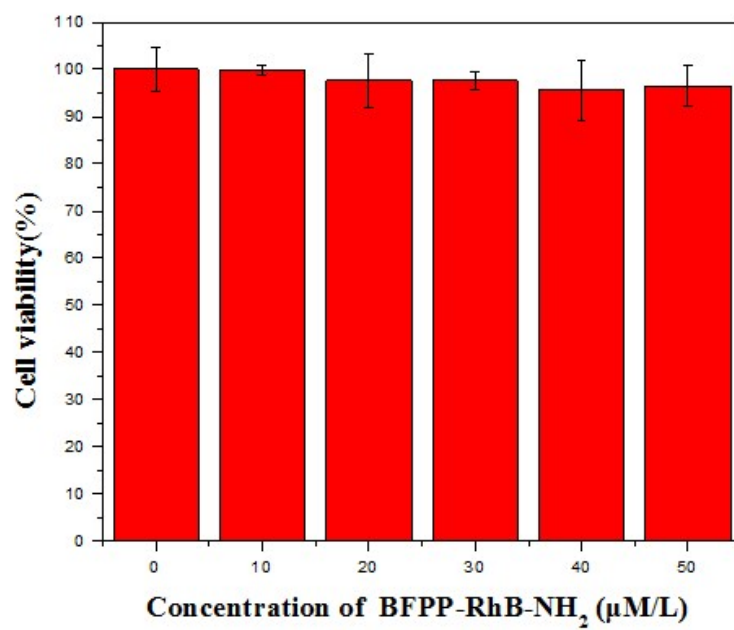


Figure S7. The *in vitro* viability of HeLa cells incubated with DFPP-RhB of different concentrations for 24 h at 37 °C.